

G-PECNET: TOWARDS A GENERALIZABLE PEDESTRIAN TRAJECTORY PREDICTION SYSTEM

Aryan Garg & Renu M. Rameshan

School of Computing and Electrical Engineering
Indian Institute of Technology, Mandi, Himachal Pradesh, India
aryangarg019@gmail.com, renum.r@gmail.com

ABSTRACT

Navigating dynamic physical environments without obstructing or damaging human assets is of quintessential importance for social robots. In this work, we solve autonomous *drone* navigation’s sub-problem of predicting out-of-domain human and agent trajectories using a deep generative model. Our method: General-PECNet or G-PECNet observes an improvement of 9.5% on the Final Displacement Error (FDE) on 2020’s benchmark: PECNet (Mangalam et al., 2020b) through a combination of architectural improvements inspired by periodic activation functions (Sitzmann et al., 2020) and synthetic trajectory (data) augmentations using Hidden Markov Models (HMMs) and Reinforcement Learning (RL). Additionally, we propose a simple geometry-inspired metric for trajectory non-linearity and outlier detection, helpful for the task. Code available at GitHub

1 INTRODUCTION

Multimodal human or pedestrian trajectory prediction is an ill-posed problem of predicting the final and intermediate steps of some or all pedestrians when only a limited context of their previous trajectories and the scene is known. This is further complicated by implicit personal values and social rules that pre-define the interaction to an extent. Autonomous navigation for robots or social agents (Bennewitz et al., 2002), can only be enabled by accurate predictions for further downstream planning tasks. For the prediction problem, we contribute twofold: a novel reinforcement learning based synthetic dataset and a variational autoencoder (Kingma & Welling, 2013) based pedestrian prediction network: General-PECNet which achieves state-of-the-art performance on the goal-point or final destination prediction error (FDE). G-PECNet is an adaptation of PECNet (Mangalam et al., 2020b), 2020’s state-of-the-art (Mangalam et al., 2020b) method.

2 RELATED WORK

We present a year-wise sorted concise summary of previous seminal pedestrian prediction networks in Tab 1. All previous works use the following 3 datasets: ETH (Pellegrini et al., 2009), UCY (Lerner et al., 2007), and Stanford Drone dataset or SDD (Robicquet et al., 2016).

3 METHOD

3.1 AUGMENTING WITH RL SYNTHETIC TRAJECTORIES

Synthetic trajectories were created using traditional Newtonian equations of motion and interaction modeling using a Hidden Markov Model. Finally, we train RL-based bots/agents deployed in the aforementioned interaction (HMM) model using Deep Policy Gradients (DPG).

DPG agents were modeled with two major goals: reaching the destination quickly and avoiding collisions with fellow agents/pedestrians. Apart from acceleration, stopping for another crossing pedestrian (being considerate) was implicitly decided by the agent’s *randomly pre-defined* sociability, fitness, and patience attributes. We add a circular proximity (fixed radius) detection mechanism to penalize agents that collide with others in the playground.

Method	Year	ADE	FDE
DESIRE (Lee et al., 2017)	2017	19.25	34.05
Social GAN (Gupta et al., 2018)	2018	27.23	41.44
Sophie (Sadeghian et al., 2018)	2019	16.27	29.38
CGNS (Li et al., 2019)	2019	15.6	28.2
CF-VAE (Bhattacharyya et al., 2020)	2019	12.60	22.30
P2TIRL (Deo & Trivedi, 2021)	2020	12.58	22.07
PECNet (Mangalam et al., 2020b)	2020	9.96	15.88
Y-Net (Mangalam et al., 2020a)	2021	7.85	11.85
V^2 -Net (Wong et al., 2022)	2022	7.12	11.39
NSP-SFM (Yue et al., 2023)	2022	6.52	10.61
G-PECNet	2022	26.75	9.04

Table 1: ADE is the average displacement error and FDE is the final displacement error. All networks are evaluated on SDD (Robicquet et al., 2016), with the total number of pedestrians to consider for predictions as 20 ($K = 20$), except ours. Our ADE (26.75) is not low as we use a decoupled PECNet; not using the social pooling layers (Alahi et al., 2016). We primarily focus on predicting the goal point of pedestrians. The intuition is that all intermediate steps could then be refined from coarser estimates after the endpoint is fixed, similar to the training procedure of denoising diffusion probabilistic models (Ho et al., 2020).

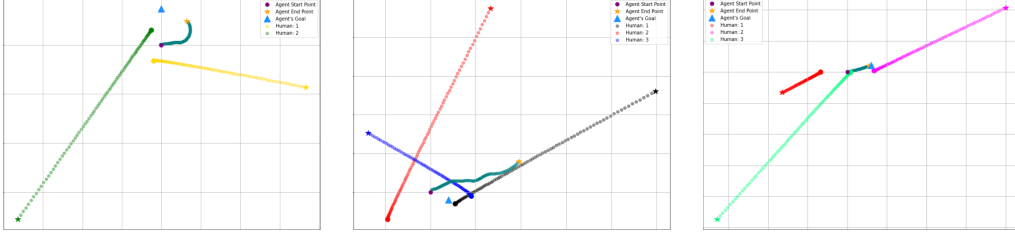


Figure 1: The RL agent is inserted and trained in an HMM interaction playground. Agent’s trajectory is turquoise. Evolution of the samples produced. First, the agent learns to turn. The second depicts a complicated scene where the agent learns to avoid multiple collisions. The last scene depicts the agent successfully avoiding a collision and reaching its goal.

Mathematically, the reward function at time step t : R_t for the agents to finally reach the goal G is defined by $R_t = AF^t (n_{ICS} + 1)^{(AS+AP)} \div t^2 (1 + \|G - x_t\|_2)$ where AF , AP , and $AS \in [0, 1]$. x_t is the agent’s current position, and n_{ICS} is the number of impending collision states. AS and AP are its sociability and patience respectively, determining its recklessness. AF : Agent’s Fitness enforces reaching the goal quickly. Finally, the loss function is the one used in standard deep-policy gradients methods: $J(\phi) = - \sum_{t=1}^N \log(P_\phi(a_t|s_t)) R_t$ where, $P(\cdot)$ is parameterized by ϕ , a simple neural network that emulates the agent’s action and state space at any time t . Training evolution is shown in figure 1.

3.2 PERIODIC ACTIVATION: SIREN IMPROVEMENT

We adapt the architecture to capture finer spatial and temporal details (Sitzmann et al., 2020) by replacing all ReLU (Agarap, 2018) activations with a simple sinusoidal function: $\mathbf{x}_i \rightarrow \phi(\mathbf{x}_i) = \sin(\mathbf{W}_i \mathbf{x}_i + \mathbf{b}_i)$, where i denotes the i^{th} layer of the neural network.

3.3 TRAJECTORY NON-LINEARITY & OUTLIER DETECTION CRITERION: ABScore

We introduce a simple criterion: Abruptness Score or *AbScore* to measure the turns and variability or non-linearity in each trajectory. An areal-scaled (bounding box area) of the metric is used for outlier detection. More details in A.3.

URM STATEMENT

The authors acknowledge that the first author of this work meets the URM criteria of ICLR 2024 Tiny Papers Track.

REFERENCES

- Abien Fred Agarap. Deep learning using rectified linear units (relu), 2018. URL <https://arxiv.org/abs/1803.08375>.
- Alexandre Alahi, Kratarth Goel, Vignesh Ramanathan, Alexandre Robicquet, Li Fei-Fei, and Silvio Savarese. Social lstm: Human trajectory prediction in crowded spaces. In *Proceedings of the IEEE Conference on Computer Vision and Pattern Recognition (CVPR)*, June 2016.
- Maren Bennewitz, Wolfram Burgard, and Sebastian Thrun. Learning motion patterns of persons for mobile service robots. In *Proceedings of the IEEE International Conference on Robotics and Automation (ICRA)*, pp. 3601–3606, 2002.
- Apratim Bhattacharyya, Michael Hanselmann, Mario Fritz, Bernt Schiele, and Christoph-Nikolas Straehle. Conditional flow variational autoencoders for structured sequence prediction, 2020.
- M. Brand, N. Oliver, and A. Pentland. Coupled hidden markov models for complex action recognition. In *Proceedings of IEEE Computer Society Conference on Computer Vision and Pattern Recognition*, pp. 994–999, 1997. doi: 10.1109/CVPR.1997.609450.
- Nachiket Deo and Mohan M. Trivedi. Trajectory forecasts in unknown environments conditioned on grid-based plans, 2021.
- Agrim Gupta, Justin Johnson, Li Fei-Fei, Silvio Savarese, and Alexandre Alahi. Social gan: Socially acceptable trajectories with generative adversarial networks, 2018.
- Jonathan Ho, Ajay Jain, and Pieter Abbeel. Denoising diffusion probabilistic models, 2020.
- Diederik P Kingma and Max Welling. Auto-encoding variational bayes, 2013. URL <https://arxiv.org/abs/1312.6114>.
- Namhoon Lee, Wongun Choi, Paul Vernaza, Christopher B. Choy, Philip H. S. Torr, and Manmohan Chandraker. Desire: Distant future prediction in dynamic scenes with interacting agents, 2017.
- Alon Lerner, Yiorgos Chrysanthou, and Dani Lischinski. Crowds by example. *Computer Graphics Forum*, 26, 2007.
- Jiachen Li, Hengbo Ma, and Masayoshi Tomizuka. Conditional generative neural system for probabilistic trajectory prediction, 2019.
- Karttikeya Mangalam, Yang An, Harshayu Girase, and Jitendra Malik. From goals, waypoints and paths to long term human trajectory forecasting, 2020a.
- Karttikeya Mangalam, Harshayu Girase, Shreyas Agarwal, Kuan-Hui Lee, Ehsan Adeli, Jitendra Malik, and Adrien Gaidon. It is not the journey but the destination: Endpoint conditioned trajectory prediction. *CoRR*, abs/2004.02025, 2020b. URL <https://arxiv.org/abs/2004.02025>.
- S. Pellegrini, A. Ess, K. Schindler, and L. van Gool. You’ll never walk alone: Modeling social behavior for multi-target tracking. In *2009 IEEE 12th International Conference on Computer Vision*, pp. 261–268, 2009. doi: 10.1109/ICCV.2009.5459260.
- A. Robicquet, A. Sadeghian, A. Alahi, and S. Savarese. Learning social etiquette: Human trajectory prediction in crowded scenes. 2016. URL http://cvgl.stanford.edu/projects/uav_data/.
- Amir Sadeghian, Vineet Kosaraju, Ali Sadeghian, Noriaki Hirose, S. Hamid Reza Tofighi, and Silvio Savarese. Sophie: An attentive gan for predicting paths compliant to social and physical constraints, 2018.

Vincent Sitzmann, Julien N. P. Martel, Alexander W. Bergman, David B. Lindell, and Gordon Wetzstein. Implicit neural representations with periodic activation functions, 2020. URL <https://arxiv.org/abs/2006.09661>.

Conghao Wong, Beihao Xia, Ziming Hong, Qinmu Peng, Wei Yuan, Qiong Cao, Yibo Yang, and Xinge You. View vertically: A hierarchical network for trajectory prediction via fourier spectrums, 2022.

Jiangbei Yue, Dinesh Manocha, and He Wang. Human trajectory prediction via neural social physics, 2023.

A APPENDIX

A.1 DEEP POLICY GRADIENT PER AGENT NETWORK

We use a simple fully connected ReLU-activated neural network (nodes: $8 \rightarrow 16 \rightarrow 8 \rightarrow 4$) with 8 inputs: current x -coordinate, current y -coordinate, x -goal, y -goal, fitness, patience, sociability, and distance to nearest person/agent and 4 output nodes defining the action space: the speed, direction, acceleration magnitude and acceleration direction to take another step. An overview of the whole workflow can be found in Fig 2.

HMMs were considered for the interaction modeling due to their high success in spatiotemporal tasks (Brand et al., 1997).

Unique Points	Trajectories	% dataset
1	145	5.13%
2	62	2.19 %
3	71	2.51 %
4	69	2.44%
5	57	2.01%
6	41	1.45%
7	51	1.80%
8	28	0.99%
9	26	0.92%
10	24	0.85%
11	22	0.78%
12	25	0.88%
13	17	0.60%
14	24	0.85%
15	22	0.78%
16	22	0.78%
17	39	1.38%
18	30	1.06%
19	76	2.69%
20	1978	69.92%

Table 2: SDD: Trajectories’ unique points. 145 trajectories had 1 unique point, i.e, the goal and starting point as the same with all other points being sampled there itself: Stationary

Based on the quantitative (table: 2), we augmented the training dataset to keep the statistical properties of the training dataset intact.

A.2 ABLATION STUDIES

We performed two ablation studies. First, by decoupling the ADE and the FDE metrics. See table 3.

Second, without the standardization parameter on the input trajectories. We note an adverse effect on ADE and a significant state-of-the-art improvement on FDE, by removing standardization. See table 4 and figure ??.

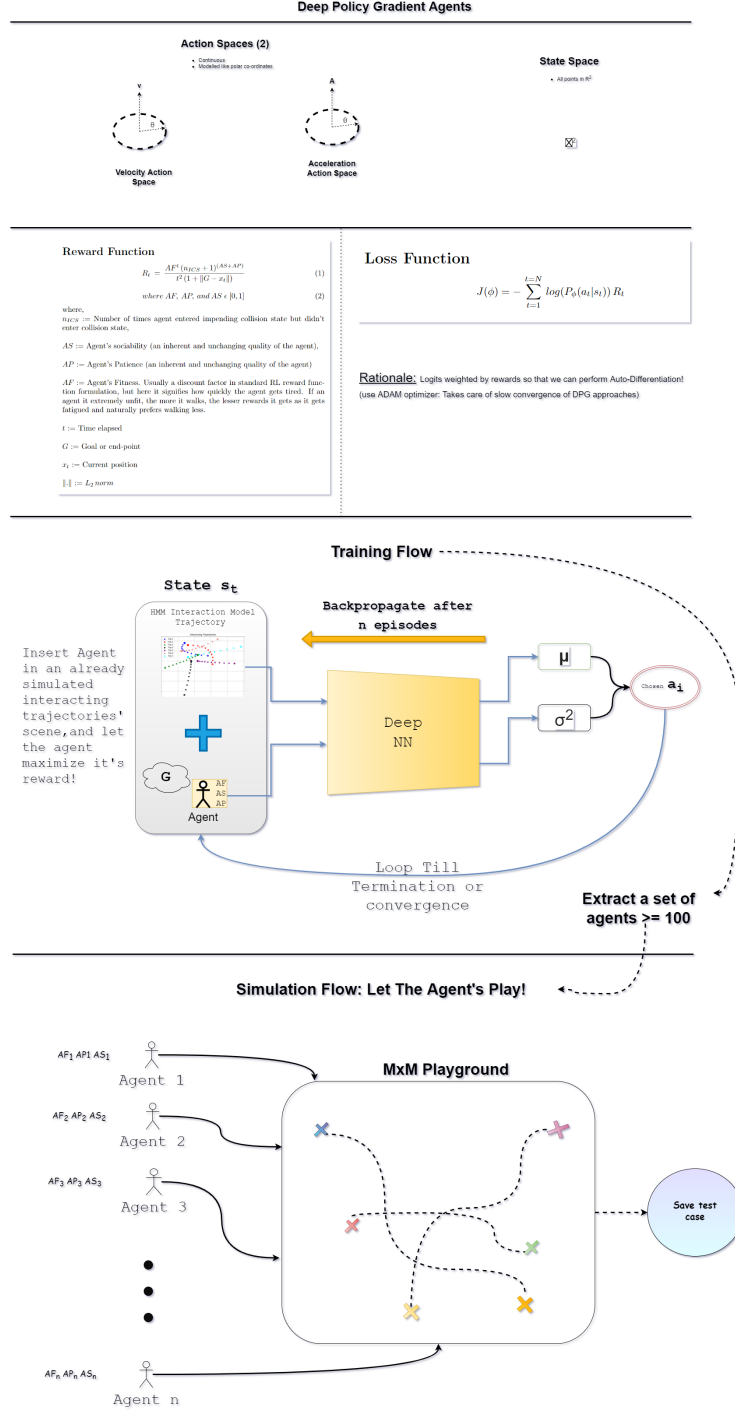


Figure 2: RL modeling

We notice an absurdity in PECNet’s codebase where the standardization parameter(= 1.86) is also dividing the ADE metric. We remove that division for G-PECNet and report fair metrics.

A.3 NON-LINEARITY ANALYSIS: ABRUPTNESS-SCORE

We clustered SDD’s trajectories (3) based on the bounding boxes to get an estimate of the maximal displacement and turn in each trajectory. Based on this information, we introduce a novel and simple

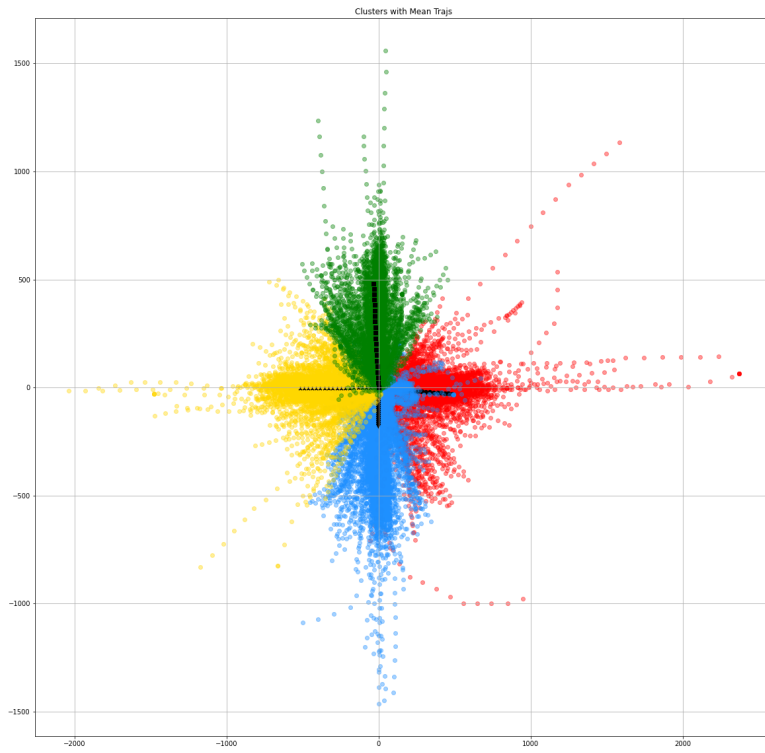


Figure 3: SDD training dataset. Frobenius norm-based clustering of trajectories, with black trajectories representing the cluster.

Learning Rate	ADE	FDE	Best FDE epoch
0.001	>50	15.68	457
0.0005	>50	15.76	301
0.0003	>50	15.9	541
0.0002	>50	15.65	420
0.0001	>50	15.92	391

Table 3: Decoupled system (ADE and FDE). No social pooling. ADE is independent of FDE.

Learning Rate	ADE	FDE	Best FDE epoch
0.001	22.20	9.32	915
0.0005	29.91	9.05	834
0.0003	25.92	9.37	998
0.0002	26.75	9.04	908
0.0001	25.57	9.05	235

Table 4: State-of-the-art FDE of G-PECNet. Modifications: Trained on augmented SDD. No Standardization. Decoupling of ADE and FDE or no social pooling usage. A higher ADE is observed due to this

metric: *Abruptness Score* to measure the turns and variability or non-linearity in each trajectory. An areal-scaled and an unscaled version of the metric is used for analysis and outlier detection. The intuition and mathematical formulation are as follows:

In the example figure 4, the trajectories $\zeta_1 = \{A, B, C1\}$ and $\zeta_2 = \{A, B, C2\}$ are shown. The dotted blue line is normal to the red danger zone. Points that fall under this danger zone will form an obtuse turn trajectory like ζ_2 . Naturally, we want the score to assign a larger value to ζ_2 than ζ_1 since the turn is huge and the trajectory (more) abruptly changes direction.

Mathematically,

$$AbScore = \left\lceil \frac{180 \cdot \theta}{10\pi} \right\rceil |\vec{a} \times \vec{b}| \quad (1)$$

where

$$\vec{a} = \vec{AB}, \vec{b} = \vec{BC} \quad (2)$$

$$\theta = \left| \arcsin \frac{|\vec{a} \times \vec{b}|}{|\vec{a}| |\vec{b}|} \right| \quad (3)$$

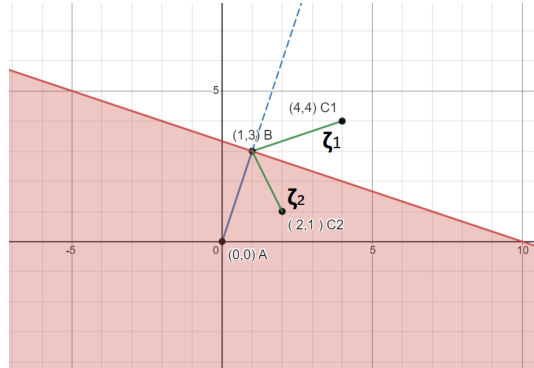


Figure 4: Defining Turns

Statistic	Value
Maximum	494866.374
Minimum	0.0
Mean	3430.665
Std. Deviation	11987.34

Table 5: Abruptness Score for non-linearity analysis of Stanford Drone Dataset

If θ is obtuse, we add $\pi/2$ to θ before sending it to equation 1.

For scaling we simply divide the abruptness score by the area of the tightest-bounding-box of the trajectory or divide by $(\max(\zeta_x) - \min(\zeta_x)) * (\max(\zeta_y) - \min(\zeta_y))$. For perfectly linear trajectories, we use the length of the trajectory for scaling.

We need areal-scaling to get an unbiased estimate of trajectories’ non-linearity that spans widely different sizes or regions. Based on this metric we analyze SDD and report that the trajectories are not non-linear on average however the distribution contains outliers with huge non-linearity scores. This analysis provided us with an estimate of the dataset’s non-linearity for synthetic dataset generation purposes. See table 5 and figure 5.

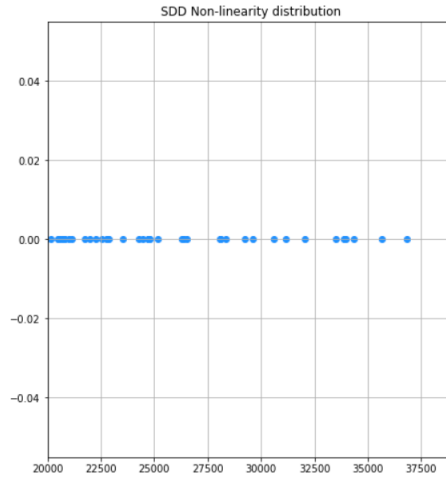


Figure 5: SDD’s Non-Linearity Distribution Tail. (Thresholded to remove outliers)